

High-temperature creep properties of uranium dioxide pellet

GAO Jia-cheng(高家诚), WANG Liang-fen(王良芬), WANG Yong(王 勇), WU Shu-fang(吴曙芳)

College of Materials Science and Engineering, Chongqing University, Chongqing 400044, China

Received 5 November 2008; accepted 6 March 2009

Abstract: High-temperature creep properties of sintered uranium dioxide pellets with two grain sizes (9.0 μm and 23.8 μm) were studied. The results indicate that the creep rate becomes a little faster with the reduction of the uranium dioxide grain size at the same temperature and the same load. At the same temperature, the logarithmic value of the steady creep rate vs stress has linear relation, and with increasing load, the steady creep rate of the sintered uranium dioxide pellet increases. Under the same load, the steady creep rate of the sintered uranium dioxide pellet increases with increasing temperature; and the creep rates of sintered uranium dioxide pellet with the grain size of 9.0 μm and 23.8 μm under 10 MPa are almost the same. The creep process is controlled both by Nabarro—Herring creep and Hamper—Dorn creep for uranium dioxide pellet with grain size of 9.0 μm , while Hamper—Dorn creep is the dominant mechanism for uranium dioxide with grain size of 23.8 μm .

Key words: uranium dioxide pellet; grain size; creep property; creep mechanism

1 Introduction

Uranium dioxide is an important ceramic mainly used as a fuel in nuclear power plants[1–3]. All uranium dioxide pellets are produced by high-temperature sintering in hydrogen atmosphere. For the thoughts of environmentalism and purpose of economizing cost, low temperature sintering of uranium dioxide pellets has become the hotspot of research since 1960s. We have primarily studied the mechanism and processes in low-temperature sintering of uranium dioxide pellets. The sintered pellets are characterized by high quality and low cost[4–9]. However, the grain size of uranium dioxide pellets by low-temperature sintering is smaller than one by high-temperature sintering technology.

The low-temperature sintering technology was not presented ever. So, the creep properties of uranium dioxide pellet sintered by this technology are unknown. Furthermore, the mechanism of uranium dioxide pellet was a focus of many studies. However, there is a great deal of disagreement in the literature. For example, based on the observation of a dependence of the creep rate on d^{-2} (d is grain size), WANG and NICH[2] and SELTZER et al[10] suggested Nabarro—Herring lattice diffusion creep as the controlling mechanisms for $d=10\text{--}27\text{ }\mu\text{m}$. In

contrast, FROST et al[11] and SOLOMON[12] proposed Coble grain boundary diffusion creep as the dominant mechanism for uranium dioxide material having $d\leq 10\text{ }\mu\text{m}$. So, in this work, the creep properties of uranium dioxide pellet with different grain sizes were measured; the results were compared; and the mechanism was also discussed.

2 Experimental

Specimens were made from a batch of uranium dioxide powder. Their density was 95% of the theoretical density of uranium dioxide pellet and the grain sizes were 9.0 μm (small grain size pellets by low-temperature sintering technique) and 23.8 μm (large grain size pellets by high-temperature sintering), respectively. All compression creep tests were conducted in a suitable furnace. The operating temperature of uranium dioxide pellet was 1 273–1 373 K, with pressure of 10 MPa in the reactor. They were performed at 20–50 MPa, 1 673 K and 1 773 K, respectively, under a nitrogen atmosphere to shorten the experimental time.

Experimental process was as follows: load samples into the furnace, vacuumize to $<0.1\text{ MPa}$, add nitrogen, heat the furnace to needed temperature; when the temperature was stable, apply load to required load, use

displacement measuring device (grating micrometer sensor, TG130/TG150A, 0.5 μm) to record the displacement; when the experiment came to the steady creep, unload and cut off the electricity, then cool with furnace. The amount of compression was calculated using the displacement, then a chart was formed with abscissa of t (time) and ordinate of the amount of compression by the least square method. The slope of line is rate of steady creep.

3 Experimental results

Table 1 shows the steady creep rate of uranium dioxide pellets with different grain sizes (9.0 μm , 23.8 μm) under 20–50 MPa at 1 673 K and 1 773 K, respectively.

Table 1 Steady creep rate of UO_2 pellets at 1 673 K and 1 773 K

Grain size/ μm	1 673 K		1 773 K	
	Stress/MPa	Steady creep rate/($10^{-4}\text{mm}\cdot\text{h}^{-1}$)	Stress/MPa	Steady creep rate/($10^{-4}\text{mm}\cdot\text{h}^{-1}$)
9.0	30	7.282 0	20	3.619 3
	40	10.900 0	30	7.429 3
	50	15.300 0	40	11.700 0
23.8	30	4.034 2	20	1.936 0
	40	9.892 1	30	4.518 7
	50	13.900 0	40	10.513 0

Creep of stoichiometric polycrystalline uranium dioxide with standard grain size is usually described in a $\lg \dot{\epsilon} - \lg \sigma$ plot (Fig.1). The limit of creep or the creep rate can be calculated using extrapolation under the same temperature.

Calculation formulae for steady creep stress and strain are described. The relationship between stress and strain for uranium dioxide (9.0 μm and 23.8 μm) at 1 673 K is listed in formulae (1) and (2), respectively, and the same relationship at 1 773 K is listed in formulae (3) and (4).

$$\lg \dot{\epsilon}_1 = 1.451 00 \lg \sigma - 5.482 92, T=1\ 673\ \text{K}, d=9.0\ \mu\text{m} \quad (1)$$

$$\lg \dot{\epsilon}_2 = 2.454 57 \lg \sigma - 6.994 75, T=1\ 673\ \text{K}, d=23.8\ \mu\text{m} \quad (2)$$

$$\lg \dot{\epsilon}_3 = 1.698 04 \lg \sigma - 5.646 67, T=1\ 773\ \text{K}, d=9.0\ \mu\text{m} \quad (3)$$

$$\lg \dot{\epsilon}_4 = 2.418 08 \lg \sigma - 3.876 01, T=1\ 773\ \text{K}, d=23.8\ \mu\text{m} \quad (4)$$

The steady creep rate is calculated when the stress is 10 MPa. The results are: $\dot{\epsilon}_1 = 0.929\ 4 \times 10^{-4}\ \text{mm/h}$, $\dot{\epsilon}_2 = 0.288\ 3 \times 10^{-4}\ \text{mm/h}$, $\dot{\epsilon}_3 = 1.125\ 6 \times 10^{-4}\ \text{mm/h}$, $\dot{\epsilon}_4 = 0.348\ 4 \times 10^{-4}\ \text{mm/h}$

Table 1 and Fig.1 show that the steady creep rate becomes a little faster with the reduction of the uranium

dioxide pellet grain size at the same temperature and the same load. At the same temperature, the logarithmic value of the steady creep rate vs stress has linear relation; and with increasing load, the steady creep rate of the sintered uranium dioxide pellets increases. Under the same load, the steady creep rate of the sintered uranium dioxide increases with increasing temperature; and the creep rates of sintered uranium dioxide with the grain sizes of 9.0 μm and 23.8 μm under the load of 10 MPa are almost the same.

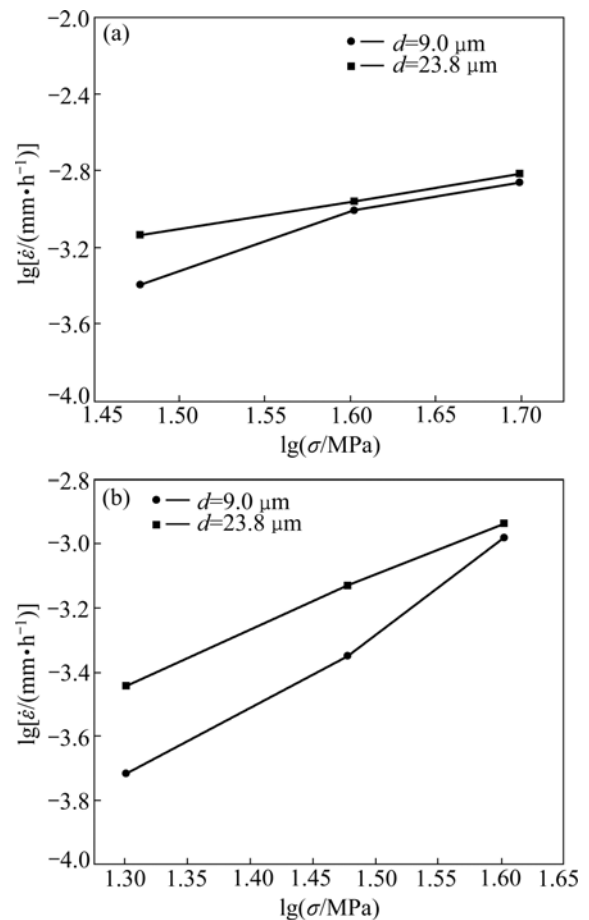


Fig.1 $\lg \dot{\epsilon} - \lg \sigma$ curves of UO_2 pellets at different temperatures: (a) 1 673 K; (b) 1 773 K

4 Mechanism discussion

The stress exponent (n) for uranium dioxide pellet with grain size of 9.0 μm is about 1.5 at 1 673 K and about 1.7 at 1 773 K. The stress exponent (n) for uranium dioxide pellet with grain size of 23.8 μm is about 2.42 at 1 673 K and about 2.44 at 1 773 K. In order to analyze the mechanism of uranium dioxide pellets, $\lg \dot{\epsilon} - \lg \sigma$ curve of experiment is compared with Nabarro—Herring creep, Coble creep and Hamper—Dorn creep.

4.1 Comparison with Nabarro—Herring creep

The mathematical model of Nabarro—Herring creep[16] is

$$\dot{\varepsilon} = A \frac{GDb}{KT} \left(\frac{b}{d} \right)^2 \left(\frac{\sigma}{G} \right) \quad (5)$$

where $\dot{\varepsilon}$ is the creep rate; K is Boltzmann's constant; $\dot{A} = B\Omega/b^3$ ($B=12-40$, $\Omega=(4/3)\pi R^3$, $R=0.080$ nm); b is Burgers vector; d is grain size; σ is stress; D is self-diffusion coefficient equal to $2 \times 10^{-19} - 5 \times 10^{-18}$ m²/s at 1 673 K and $1.0 \times 10^{-17} - 1.0 \times 10^{-16}$ m²/s at 1 773 K; Q is the activation energy equal to about 544 kJ/mol. Two formulae are deduced using above data:

At 1 673 K,

$$\dot{\varepsilon} = A \frac{GDb}{KT} \left(\frac{b}{d} \right)^2 \left(\frac{\sigma}{G} \right) = \frac{2.12 \times 10^{-17} \sigma}{d^2} \quad (6)$$

At 1 773 K,

$$\dot{\varepsilon} = A \frac{GDb}{KT} \left(\frac{b}{d} \right)^2 \left(\frac{\sigma}{G} \right) = \frac{1.00 \times 10^{-16} \sigma}{d^2} \quad (7)$$

The steady-creep rates of this creep model are shown in Table 2.

4.2 Comparison with Coble creep

The mathematical model of Coble creep is

$$\dot{\varepsilon} = A \frac{GDb}{KT} \left(\frac{b}{d} \right)^3 \left(\frac{\sigma}{G} \right) \quad (8)$$

where A is a constant equal to 50; D is boundary diffusion coefficient, $D=D_0 \exp[-Q/(RT)]$; D_0 is the grain boundary diffusion energy coefficient under standard condition; Q is the grain boundary diffusion activation energy equal to about 377 kJ/mol; other parameters are expressed as formula (5). Two formulae are deduced using above data:

At 1 673 K,

$$\dot{\varepsilon} = A \frac{GDb}{KT} \left(\frac{b}{d} \right)^3 \left(\frac{\sigma}{G} \right) = 1.75 \times 10^{-6} \exp\left(\frac{-377\,000}{8.314T}\right) \frac{\tau}{Td^3} \quad (9)$$

At 1 773 K,

$$\dot{\varepsilon} = A \frac{GDb}{KT} \left(\frac{b}{d} \right)^3 \left(\frac{\sigma}{G} \right) = 1.03 \times 10^{-5} \exp\left(\frac{-377\,000}{8.314T}\right) \frac{\tau}{Td^3} \quad (10)$$

The steady creep rate of this creep model is also shown in Table 2.

4.3 Comparison with Hamper—Dorn creep

The mathematical model of Hamper—Dorn creep is

$$\dot{\varepsilon} = A \frac{GDb}{KT} \left(\frac{\sigma}{G} \right) \quad (11)$$

where A is a constant equal to 7×10^{-11} ; other parameters are expressed as formula (5). Two formulae are also deduced using above data:

At 1 673 K,

$$\dot{\varepsilon} = A \frac{GDb}{KT} \left(\frac{\sigma}{G} \right) = 9.94 \times 10^{-6} \sigma \quad (12)$$

At 1 773 K,

$$\dot{\varepsilon} = A \frac{GDb}{KT} \left(\frac{\sigma}{G} \right) = 4.69 \times 10^{-5} \sigma \quad (13)$$

The steady creep rate of this creep model is also shown in Table 2.

The logarithms of the steady creep rate and stress in Table 2 are calculated, and then $\lg \dot{\varepsilon} - \lg \sigma$ curves are drawn and compared with the experimental results in Fig.2.

It can be seen from Fig.2, experimental results of

Table 2 Creep rates calculated in this experiment and other creep models

Temperature/ K	Grain size/ μm	Stress/ MPa	Creep rate			
			Experiment	Nabarro—Herring	Coble	Hamper—Dorn
1 667	9.0	30	7.282 0	7.881 2	0.729 1	2.976 7
		40	10.90 0	10.50 8	0.972 1	3.968 9
		50	15.30 0	13.13 5	1.215 1	4.961 1
	23.8	30	4.034 2	1.126 9	0.039 4	2.976 7
		40	9.892 1	1.502 6	0.052 6	3.968 9
		50	13.90 0	1.878 3	0.065 8	4.961 1
1 773	9.0	20	3.619 3	24.78 9	12.45 0	9.385 0
		30	7.429 3	37.18 3	18.68 8	14.07 8
		40	11.70 0	49.57 8	24.90 0	18.77 0
	23.8	20	1.936 0	3.544 8	0.673 3	9.385 2
		30	4.518 7	5.317 2	1.009 9	14.07 8
		40	10.51 3	7.089 5	1.346 5	18.77 0

uranium dioxide pellet with the grain size of 9.0 μm correspond to the theoretical values of Nabarro—Herring creep; while those of uranium dioxide pellet with the grain size of 23.8 μm accord with the theoretical values of Hamper—Dorn creep.

By combining with Nabarro—Herring creep and Hamper—Dorn creep, a new formula which corresponds to the experimental result is proposed:

$$\begin{cases} \dot{\epsilon} = M\dot{A}\frac{GDb}{KT}\left(\frac{b}{d}\right)^2\left(\frac{\sigma}{G}\right) + N\dot{A}\frac{GDb}{KT}\left(\frac{\sigma}{G}\right) \\ M + N = 1 \end{cases} \quad (14)$$

where M and N are coefficients; $\dot{\epsilon}$ is the steady creep rate of experiment. Values of M and N are calculated and listed in Table 3.

Table 3 shows that the creep process is controlled both by Nabarro—Herring creep and Hamper—Dorn creep for uranium dioxide with grain size of 9.0 μm . The Hamper—Dorn creep is predominate, which is ascribed to diffusion mechanisms. While it is controlled by Hamper—Dorn creep for uranium dioxide with grain size of 23.8 μm , which is ascribed to grain boundary sliding. It is similar to the results of Fig.2.

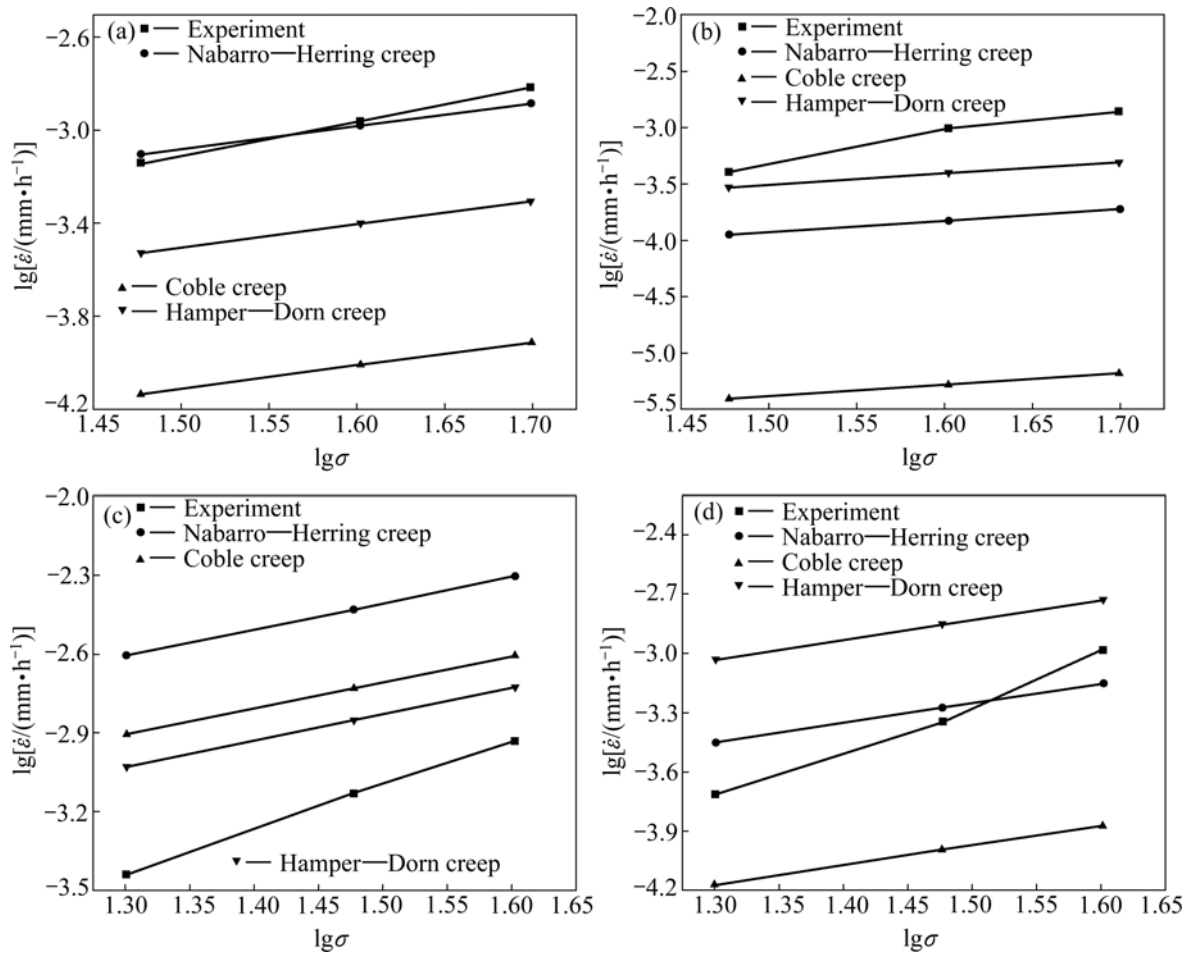


Fig.2 Comparison of $\lg \dot{\epsilon} - \lg \sigma$ between experiment and creep models: (a) 1 673 K, 9.0 μm ; (b) 1 673 K, 23.8 μm ; (c) 1 773 K, 9.0 μm ; (d) 1 773 K, 23.8 μm

Table 3 Values of M and N

Grain size/ μm	M						Average
	M_1	M_2	M_3	M_4	M_5	M_6	
9.0	0.877 80	1.059 90	1.260 00	−0.374 30	−0.287 80	−0.229 40	0.3844 00
2.8	−0.571 50	−2.401 70	−2.899 60	1.275 50	1.091 14	0.706 90	−0.466 60
Grain size/ μm	N						Average
	N_1	N_2	N_3	N_4	N_5	N_6	
9.0	0.122 20	−0.059 90	−0.260 00	1.374 30	1.287 80	1.229 40	0.615 60
2.8	1.571 50	3.401 60	3.899 60	−0.275 50	−0.091 14	0.293 10	1.466 60

5 Conclusions

1) The creep rate becomes a little faster with the reduction of the UO_2 grain size at the same temperature and the same load.

2) At the same temperature, the logarithmic value of the steady creep rate vs stress has linear relation; and with increasing the load, the steady creep rate of the sintered UO_2 pellets increases.

3) Under the same load, the steady creep rate of the sintered UO_2 increases with increasing temperature.

4) The creep rates of sintered UO_2 with the grain sizes of 9.0 μm and 23.8 μm under the load of 10 MPa are almost the same.

5) The creep process is controlled by both Nabarro—Herring creep and Hamper—Dorn creep for uranium dioxide with grain size of 9.0 μm ; while Hamper—Dorn creep is the dominant mechanism for uranium dioxide with grain size of 23.8 μm

References

- [1] DHERBEY F, LOUCHET F, MOCELLIN A. Elevated temperature creep of polycrystalline uranium dioxide: From microscopic mechanisms to macroscopic behavior [J]. *Acta Materialia*, 2002, 50(6): 1495–1505.
- [2] WANG J N, NICH T G. A new interpretation of the mechanisms in Newtonian creep of uranium dioxides [J]. *Journal of Nuclear Materials*, 1996, 228: 141–147.
- [3] GAO Jia-cheng, YANG Xiao-dong, LI Rui. Low temperature sintering mechanism on uranium dioxide [J]. *Journal of Materials Science*, 2007, 42(10): 33–38.
- [4] YANG Xiao-dong. Technological research on low-temperature sintering of uranium dioxide pellets [D]. Chongqing: Chongqing University, 2004: 1–4. (in Chinese)
- [5] RUELLO P, CHIRLESAN G, PETOT-ERVAS G, PETOT C, DESGRANGES L. Chemical diffusion in uranium dioxide-influence of defect interactions [J]. *Journal of Nuclear Materials*, 2004, 325: 202–209.
- [6] YUN Y, KIM H, KIM H, PARK K. Atomic diffusion mechanism of Xe in UO_2 [J]. *Journal of Nuclear Materials*, 2008, 378(1): 40–44.
- [7] BROCKZKOWSKI M E, NOEL J J, SHOESMITH D W. The influence of temperature on the anodic oxidation/dissolution of uranium dioxide [J]. *Electrochimica Acta*, 2007, 52(25): 7386–7395.
- [8] KUPRYAZHKIN A Y, ZHIGANOV A N, RISOVANY D V, NEKRASSOV K A, RISOVANY V D, GOLOVANOV V N. Simulation of diffusion of oxygen and uranium in uranium dioxide nanocrystals [J]. *Journal of Nuclear Materials*, 2008, 372: 233–238.
- [9] ZHAO Yun-feng, CHEN Jing. Studies on the dissolution kinetics of ceramic uranium dioxide particles in nitric acid by microwave heating [J]. *Journal of Nuclear Materials*, 2008, 373: 53–58.
- [10] SELTZER M S, WRIGHT T R, SPEIDEL E O. Creep behavior of low-density uranium carbide-base alloys [J]. *Journal of Nuclear Materials*, 1975, 55(3): 327–334.
- [11] FROST H J, SAEPEN F, ASHBY M F. A second report on tilt boundaries in hard sphere F.C.C. crystals [J]. *Scripta Metallurgica*, 1982, 16(10): 1165–1170.
- [12] SOLOMON A A, YUST C S, PACKAN N A. Primary creep of uranium dioxide and effect of amorphous grain boundary phases [J]. *Materials Science and Engineering A*, 1995, 191(1/2): 135–141.

(Edited by YANG Hua)